Multivalent polymer-grafted nanoparticles as reinforcing fillers for 3D printable self-healing elastomers

Griffen J. Desroches¹, Carl J. Thrasher^{2*}, Nicholas S. Diaco³, Ibrahim O. Raji⁴, Dominik Konkolewicz⁴, A. John Hart³, Robert J. Macfarlane^{2*}

¹Department of Chemistry, Massachusetts Institute of Technology, 77 Massachusetts Avenue, Cambridge, Massachusetts 02139, United States

²Department of Materials Science and Engineering, Massachusetts Institute of Technology, 77
Massachusetts Avenue, Cambridge, Massachusetts 02139, United States

³Department of Mechanical Engineering, Massachusetts Institute of Technology, 77

Massachusetts Avenue, Cambridge, Massachusetts 02139, United States

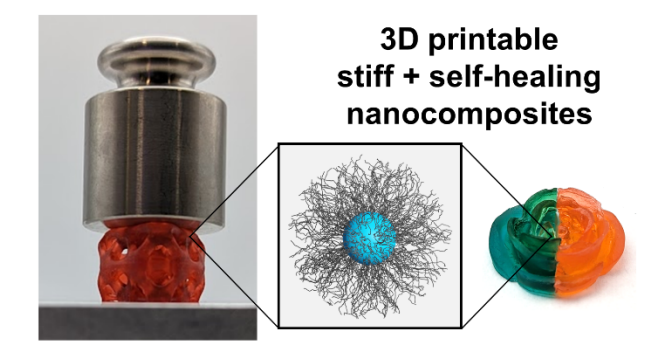
⁴Department of Chemistry and Biochemistry, Miami University, 651 E. High St., Oxford, OH 45056, United States

Keywords: Elastomers, nanoparticles, nanocomposite materials, polymer particles, mechanical properties, self-healing, 3D printing

Corresponding Author Emails: cthrash@mit.edu, rmacfarl@mit.edu

Abstract

3D printable elastomers capable of self-healing are attractive for fabricating complex biomimetic and soft-robotic devices. While polymer network reorganization can be enabled with dynamic bond exchange, this strategy typically faces intrinsic tradeoffs between healability, processability, and mechanical performance. Thus, new material design strategies that can subvert these tradeoffs are needed. Here, we report the use of multivalent polymer-grafted nanoparticles (PGNPs) as reinforcing fillers for self-healing photoresins. As each nanoparticle is functionalized with thousands of polymer chains engaging in multivalent interactions with the surrounding elastomeric matrix, the bulk modulus of the composite can be increased without impairing the local segmental motion of polymer chains necessary for self-healing. We also examine PGNP structural parameters to establish structure-property relationships that permit fine-tuning of composite mechanical performance. Finally, these enhancements do not impair the materials' manufacturability, as they can be used as feedstocks for digital light printing to produce complex and high-resolution 3D objects.



Elastomeric materials that can heal after experiencing mechanical damage are of significant interest for use in complex soft devices in fields such as biomedicine and soft robotics. ^{1–3} However, modifying the composition of an elastomer to impart self-healing capacity typically comes at the expense of mechanical properties. ^{4–7} For example, the incorporation of large quantities of weak, reversible crosslinks (e.g. supramolecular bonds) can facilitate self-healing via molecular reassociation. ⁸ However, a reliance on many weak crosslinks tends to make materials vulnerable to creep. ^{9,10} Conversely, good self-healing can also be achieved with smaller quantities of stronger reversible crosslinks (e.g. 1-2% of dynamic covalent bonding groups), but only if the polymer network is soft enough to allow long-range polymer motion. ^{11,12} Thus, most strategies to impart self-healing to elastomers exhibit an intrinsic trade-off between modulus and healing capacity that limits the practical utility of many conventional self-healing polymer materials. ^{13–16}

The task of achieving both strong and healable polymer materials is made even more difficult by requirements for processability. Notably, many of the most pertinent uses of self-healing elastomers benefit from the fabrication of complex 3D shapes using techniques like additive manufacturing (AM), particularly vat photopolymerization (VP).^{1,2,17} VP involves the iterative, layerwise illumination of patterned light into a vat of photoactive resin and is ideal for 3D printing materials with controlled chemical composition as it polymerizes from liquid-phase feedstocks.¹⁸ Despite its potential, the design of VP-compatible elastomeric resins is non-trivial, as constraints on viscosity, resin chemistry, and photopolymerization environment typically result in lowered conversion rates and reduced polymer molecular weights that hinder mechanical performance.^{19–21} The synthesis of photopolymers that balance printability, capacity for self-healing, and controlled mechanical properties requires is thus a complicated challenge.

Some methods to simultaneously enhance healing and modulus in printed polymer networks have been explored with moderate success, indicating potential routes forward in addressing this difficulty. For example, fast exchanging weak bonds (i.e. hydrogen bonds) can be combined with dynamic covalent chemistries to reinforce a loosely crosslinked material. ^{22–24} The use of dynamic crosslinks can impart increased modulus and toughness while retaining healing capacity, but generally with the drawback of making the materials viscoelastic, thereby limiting the range of potential application. Alternatively, plasticizing molecules can be incorporated to add polymer mobility, which has been shown to yield windows of synergy where both toughness and healing are enabled. ^{13,25} However, even in these cases, the intrinsic tradeoff between modulus and mobility largely remains. A separate emerging strategy to enhance self-healing materials involves the use of nanoscale additives to modulate polymer network connectivity and polymer chain motion. ^{26–28} While initial approaches are promising, additional exploration of structure-property relationships in these nanocomposite materials is needed to alleviate challenges such as colloidal stability, rheological compatibility with AM, and synthetic scale. ^{29–32}

We hypothesized that many of these challenges could be addressed by using polymer grafted nanoparticles (PGNPs) as additives in 3D printable self-healing resins. Prior investigations on thermosetting polymers and polymer adhesives have shown that PGNPs with long-chain polymer brushes capable of interacting via entanglement, hydrogen bonding, and ionic interactions can act as multivalent supramolecular crosslinkers, strengthening polymer networks without inhibiting the polymer mobility needed for adhesion.³³ Further, because polymer graft composition can be used to enhance PGNP compatibility with a matrix resin, PGNP fillers could be more readily integrated into VP additive manufacturing processes than unfunctionalized or small-molecule ligand coated particles.

We show that multivalent PGNP additives can enhance the strength of self-healing photoelastomers without reducing self-healing capacity. Specifically, we examined PGNP addition to resins that use a small number of thermally activated retro thiol-Michael reactions to self-heal, as previous elastomers employing this chemistry (in the absence of PGNP additives) showed the typical tradeoff between modulus and healing capacity.²⁵ By tailoring PGNP design parameters (e.g. polymer brush length, particle size, volume fraction), we demonstrate that the modulus of a given resin composition can be substantially enhanced while retaining the ability to self-heal. These PGNP-filled resins showed significant extensibility (300-700% strain), repeated healings (3+ cycles) with minimal loss of healing capacity, and up to a 3x increase in modulus at 100% strain compared to unfilled elastomers of the same design. Additionally, control experiments using unfunctionalized nanoparticle fillers emphasized the necessity of multivalent polymer grafts in imparting mechanical strength at low filler loadings, providing insight into the mechanisms

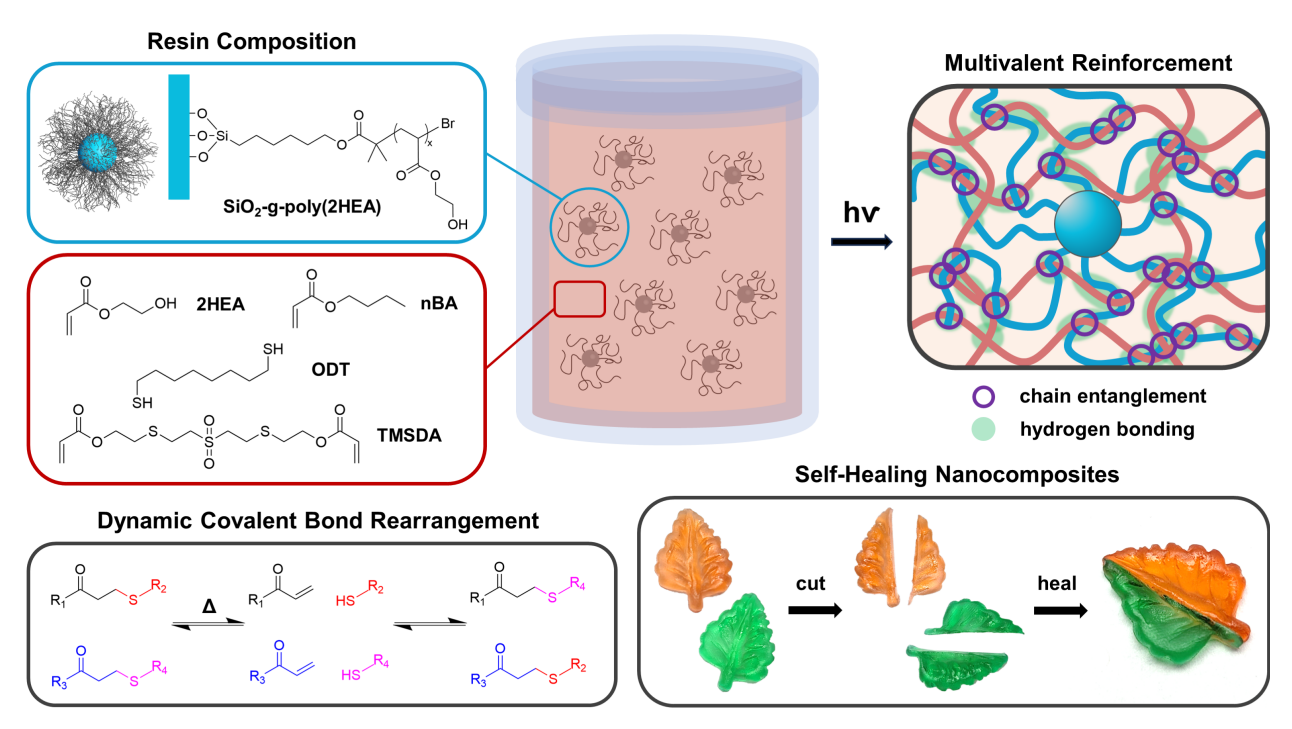


Figure 1. Resin composition (top left) and conceptual scheme of multivalent reinforcement from PGNP incorporation (top right). By exploiting dynamic covalent bond rearrangement (bottom left), PGNP-strengthened nanocomposites can heal from incurred damage (bottom right).

Table 1. Resin and PGNP Compositions

Resins						
Formulation		$TMSDA^a$		1,8-Octanedithiol ^a		$BAPO^a$
A		0		0		0.5
В		1		0		0.5
С		1		1		0.5
PGNPs						
Designation	SiO_2 Diameter $(nm)^b$			$\frac{DP}{}$ (eq.) ^c	% SiO ₂ (wt%) ^d	
50-g-100	54 ± 8		100		66.8	
50-g-190	54 ± 8		187		56.1	
50-g-1200	54 ± 8		1214		26.3	
160-g-160	164 ± 7			164		83.5

^aListed as parts per hundred rubber (phr)

through which PGNPs impart these beneficial combinations of properties. Finally, the printability of the nanocomposite resins was demonstrated using a conventional VP platform to fabricate objects with complex 3D geometry. Collectively, these results demonstrate that PGNP additives can be used to subvert typical tradeoffs between modulus and polymer flow in self-healing elastomers, providing a new strategy in the development of 3D-printable materials for self-healing structures and devices.

As a starting point, polymer-grafted nanoparticles (PGNPs) were designed to be compatible with previously reported 3D printable self-healing elastomer materials that have desirable mechanical performance (Figure 1).^{15,25} The base polymer for these resins was a statistical copolymer of 2-hydroxyethyl acrylate (2HEA) and n-butyl acrylate (nBA) monomers in an 80:20 ratio by weight (Formulation A). To prepare compatible PGNPs, poly(2-hydroxyethyl acrylate) (PHEA) polymer brushes were grown from the surface of SiO₂ nanoparticles via surface initiated ATRP.^{34–36} For all samples in this work, PGNP composition is denoted with the shorthand *X-g-Y*, where *X* is the

^bAs determined by electron microscopy

^cDegree of Polymerization, estimated from ¹H-NMR conversion

^dAs determined by thermogravimetric analysis

diameter of the core SiO₂ nanoparticle in nanometers and Y is the estimated polymer graft chain length in monomer units (Table 1). With grafting densities estimated between 0.1-0.5 chains/nm², each PGNP brush consists of thousands of PHEA chains grafted to each SiO₂ core.^{33,34,37,38} PHEA grafts ensure the colloidal stability of PGNPs in the resin suspension, as the brush chain compositions are miscible in the resin monomers. Post-polymerization, PHEA grafts interact with the polymer matrix via entanglement and hydrogen bonding of hydroxy groups through thousands of grafts all tethered to a common core, thereby providing highly multivalent non-covalent reinforcement.

Alone, Formulation A (acrylate monomers only) resin forms a soft elastomer with no intrinsic mechanism for self-healing other than self-adhesion (i.e., the formation of new hydrogen bonds and/or chain entanglements at the interface where damaged surfaces are rejoined). Modifying Formulation A by incorporating 1 part per hundred rubber (phr) of crosslinker sulfonylbis(ethane-2,1-diyl)bis(sulfanediyl)bis(ethane-2,1-diyl) diacrylate (TMSDA) adds dynamic covalent bonds that can exchange by thermally-induced retro-Michael reactions; this combination is denoted as Formulation B. However, while this network is in principle reconfigurable, the actual self-healing capacity is quite limited because the additional crosslinking density from TMSDA constricts polymer chain mobility. To enhance the healing capacity of Formulation B, a difunctional chain transfer agent 1,8-octanedithiol (ODT) was added at 1 phr (Formulation C). The addition of thiol groups to free radical acrylate polymerizations causes early chain termination events followed by reinitiation at the thiol. The incorporation of bifunctional ODT therefore broadens the molecular weight distribution of the final polymer network, simultaneously softening and plasticizing the elastomer material to enhance polymer mobility and capacity for strain.²⁵ Indeed, tensile testing of Formulation C samples showed lower modulus, higher strain at failure, and near-complete

recovery of tensile properties relative to Formulations A and B, which exhibited very limited healing capacity (Figure 2). This tradeoff between modulus and mobility is typical of self-healing systems that use a small number of dynamic groups to enable bond reconfiguration.

We hypothesized that, even though the PGNP chains do not possess functional groups capable of participating in the dynamic thiol-Michael bond exchange, the brushes would increase the stiffness of the elastomer by generating a large number of non-covalent crosslinks (entanglements and hydrogen bonds) with the surrounding polymer matrix without impeding the dynamic covalent

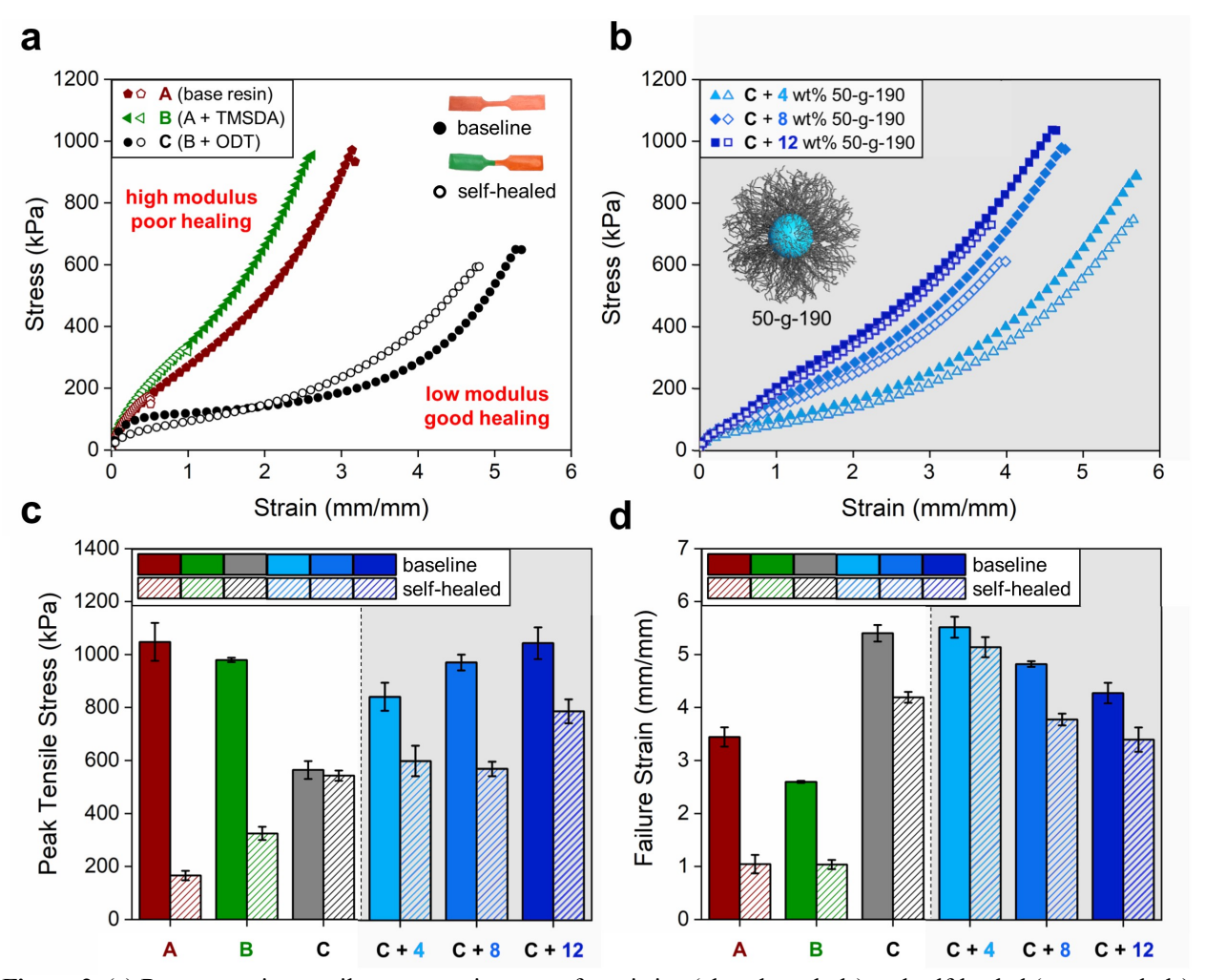


Figure 2. (a) Representative tensile stress-strain curves for pristine (closed symbols) and self-healed (open symbols) elastomers of various formulations without PGNPs. (b) Representative tensile stress-strain curves for pristine (closed symbols) and self-healed (open symbols) samples of Formulation C with various loadings of PGNP 50-g-190. (c) Average tensile strength and (d) average failure strains for the different compositions and conditions shown. All self-healed samples fractured at the cut interface.

reactions enabling network reconfiguration. We have previously demonstrated similar polymer network strengthening behavior in pressure-sensitive adhesives,³³ where ~2-3 wt% of PGNP additives increased the shear strength of the materials by as much as 33% without affecting their adhesion.

To test the ability of PGNPs to mechanically reinforce soft self-healing elastomers, a series of dog bone specimens were prepared from Formulation C with 4, 8, and 12 wt % PGNP (50-g-190) content (Figure 2b). The addition of PGNPs progressively increased the modulus and ultimate strength of dog bone samples, with a maximum strength exceeding 1 MPa at 12 wt% PGNP loading (Figure 2c). While the ultimate strains of these samples decreased with PGNP contents above 4 wt%, elongations were still well over 400% strain before failure for all samples examined (Figure 2d). Self-healing tests were conducted by cutting dog bones perpendicular to their length, placing them back together, and heating at 90 °C for 24 hours. Crucially, the self-healed performance (as measured by the peak tensile stress post-healing) upon the addition of PGNPs was largely maintained and in many cases even improved over Formulation C without PGNPs, despite the increased stiffness of the PGNP-containing materials. These properties demonstrate how the multivalent reinforcement from embedding PGNPs into a polymer network can subvert tradeoffs between stiffness and healing capacity typically observed in self-healing materials.

To examine the proposed mechanisms by which PGNPs impart improvements to self-healing elastomer performance, control experiments were performed. To verify that mechanical reinforcement was attributable to the supramolecular interactions of PGNP brushes within the matrix resin (and not simply the presence of a large particle additive), Formulation C was prepared with 2.2 wt% bare SiO₂ particles (silanol functionalized, of equal particle count to 4 wt% 50-g-190) and the tensile performance of uncut and self-healed samples were evaluated (Figure S3).

Notably, the mechanical properties of the uncut and self-healed samples with bare SiO₂ did not differ from the unreinforced Formulation C samples. The identical mechanical performance of these two samples is consistent with the hypothesis that PGNPs reinforce the elastomer matrix via multivalent non-covalent interactions with the polymer brush. To confirm that PGNP filled materials facilitated self-healing via dynamic bond exchange and not increased adhesion, a series of dog bones with various loadings of PGNP 50-g-190 were prepared using the non-dynamic covalent crosslinker 1,6-hexanediol diacrylate (HDDA) in place of TMSDA (Formulations D and E, see supporting information for details). The self-healing capacity of the non-dynamic HDDA-crosslinked elastomers was greatly reduced compared to elastomers with dynamic TMSDA crosslinks, and was further decreased when PGNPs were added to the resin (Figures S1 and S2). Thus, the self-healing performance of PGNP-containing samples can be mostly attributed to dynamic bond exchange, supporting the notion that the multivalent supramolecular reinforcement imparted by PGNPs does not significantly inhibit the long-range polymer motion required for chain reorganization.

To investigate the role of PGNP architecture in controlling the non-covalent crosslink formation enabling improved modulus and self-healing, a series of PGNPs with varied compositions (i.e. particle diameter, polymer brush length) were synthesized while the mass of SiO₂ was held at 2.2 wt% for each composite sample (Figure 3a). Increasing polymer brush chain lengths from 190 to 1200 monomer units led to substantial stiffening, likely due to the greater fraction of polymer length that is in the semi-dilute regime and can contribute to entanglement (Figure 3b, red). However, greater entanglement likely decreases the polymer network's ability to quickly

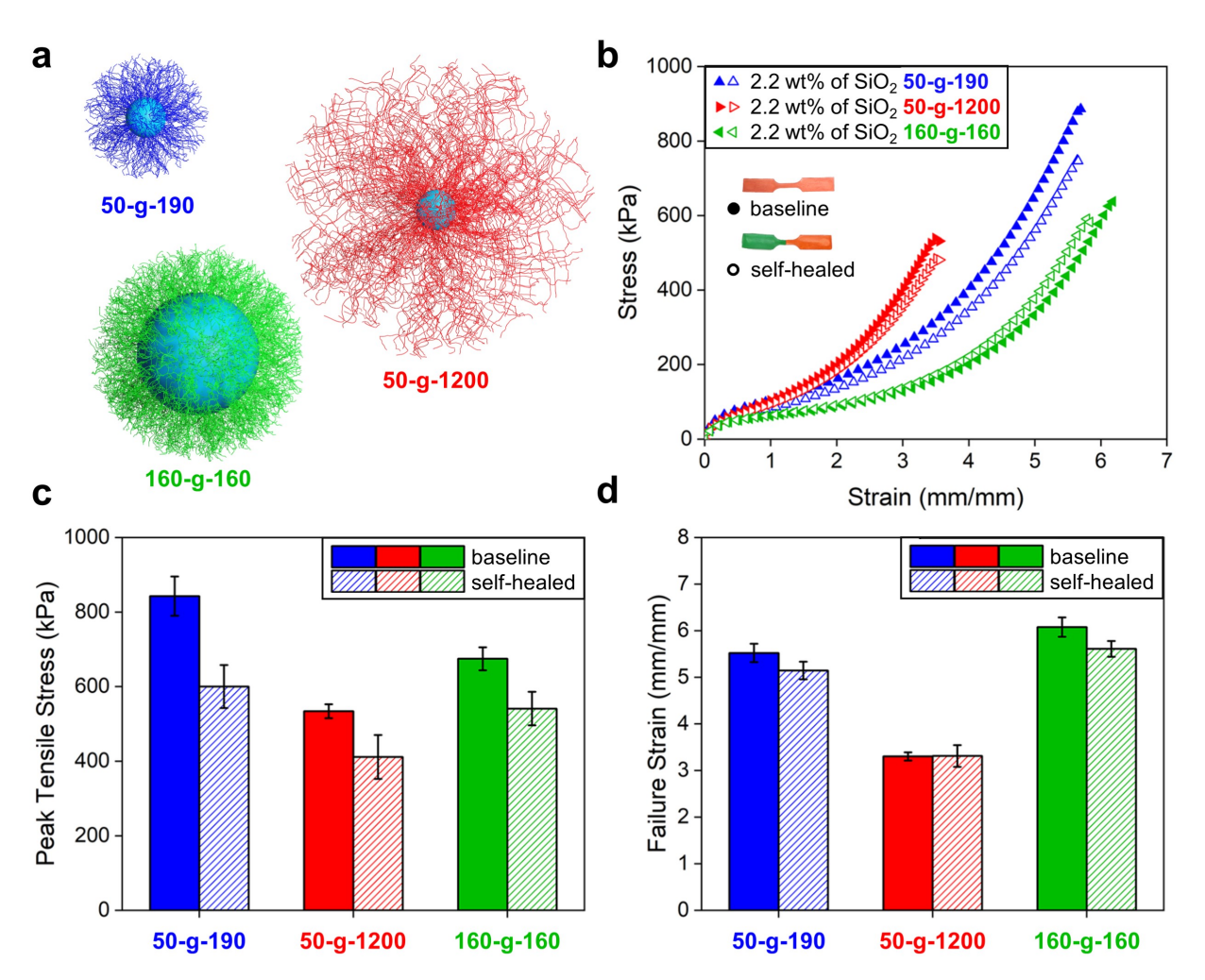


Figure 3. (a) Schematic depiction of PGNP structures with different particle sizes/brush lengths. (b) Representative stress-strain curves for Formulation C resins containing 2.2 wt% of SiO₂ PGNPs of composition 50-g-190 (blue), 50-g-1200 (red), and 160-g-160 (green). Filled and unfilled symbols indicate uncut and cut/healed samples respectively. (c) Average peak tensile stresses and (d) average failure strains for each composition and condition. All self-healed samples fractured at the cut interface.

reorganize under strain, as these samples were more prone to fracture and exhibited ~35% reduction in ultimate stress and strain (Figures 3c and 3d). Conversely, increasing core nanoparticle size to from 50 nm to 160 nm while maintaining polymer brush length resulted in softer and more extensible polymer networks (Figure 3b, green). This softening is consistent with reported literature on nanocomposites with hydrogen-bonding fillers, which can show regimes of decreasing stiffness with added filler.^{38,39} We hypothesize that the relatively limited brush-matrix interactions from short brushes do not compensate for the matrix-matrix interactions that are lost due to displacement by larger particle cores. Notably, at these PGNP loadings, all elastomers exhibited near perfect recovery of tensile properties upon healing, demonstrating that PGNP structure can be a useful design handle to modulate the mechanical properties of self-healing elastomers without adjusting PGNP filler loading.

The ability of PGNP nanocomposites to subvert tradeoffs between stiffness and self-healing make them ideal for applications where healable materials must maintain their macroscopic form during operation (e.g., soft robotics). Thus, it is also critical to ensure that these PGNP nanocomposites are compatible with manufacturing methods capable of producing complex 3D geometries. To this end, PGNP-loaded resins (4 wt% of 50-g-100 PGNPs) were used as feedstocks in a digital light processing (DLP) 3D printer. Resins were colored with either red or green food dye to reduce light-scattering and printed into complex objects such as the benchmark "3Dbenchy" boat⁴⁰ (Figure 4a) and a curved octet truss (Figure 4b). Importantly, loaded resins were found to be colloidally stable for hours, printable with no changes to print parameters from resins without PGNPs, and indistinguishable from Formulation C control resins by eye after printing. Static loading of a printed 1.5 g octet truss under a 100 g weight showed minimal compressive strain (~5-10%) and responsive elastic recovery, demonstrating a practical degree of stiffness (Figure

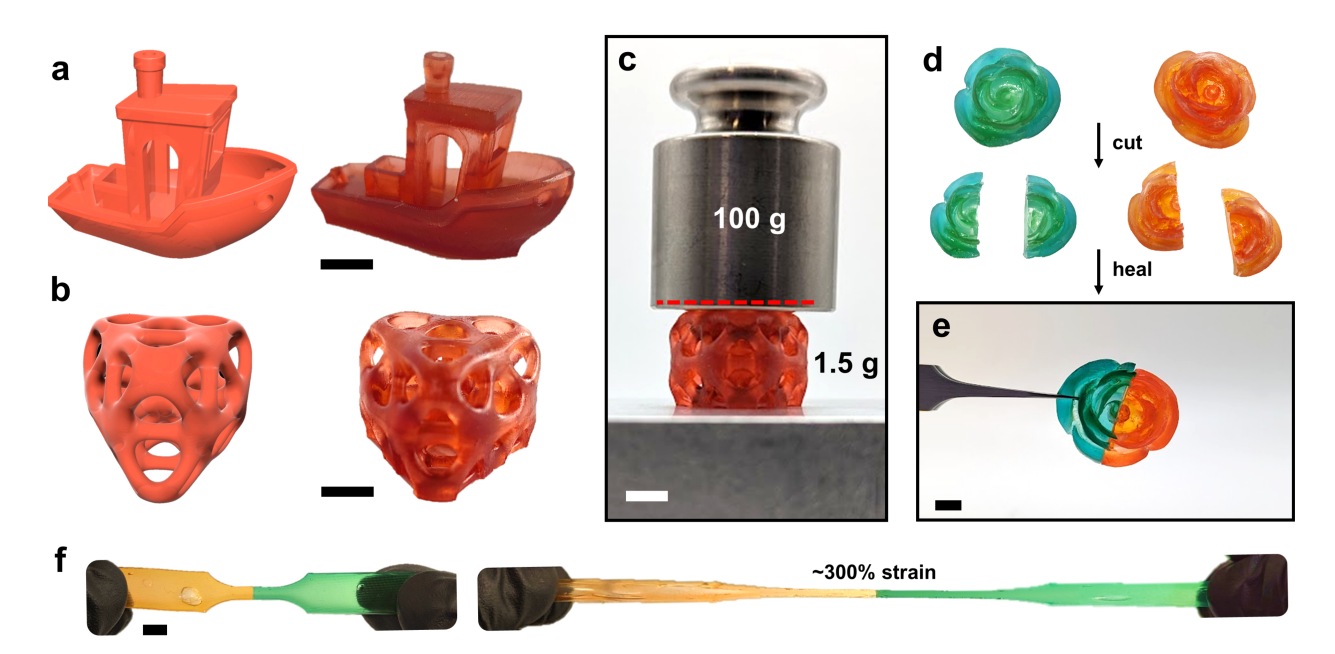


Figure 4. (a,b) 3D models and printed objects of Formulation C resins with 4 wt% 50-g-100 PGNPs representing (a) "3DBenchy" and (b) a curved octet truss. (c) Printed octet truss (1.5 g) under the compression of a 100 g weight deflects 5-10% (original height marked by dotted red line). (d,e) Scheme showing healing process of geometrically complex parts. (f) Elongation of a PNGP-loaded dogbone post healing. Scale bars are 5 mm.

4c). Flower and dog bone structures (Figure 4d,e,f) were used to illustrate the healability of printable PNGP nanocomposite resins, and each of these geometries was able to be cut and reconnected using the same protocols examined for the samples above (Fig. 2). Importantly, these more complex geometries remained free-standing (Fig. 2e) and stretchable (Fig. 2f) after healing. These demonstrations illustrate how PGNP reinforcement of printable self-healing materials provides a simple strategy to manufacture relatively stiff elastomers with good self-healing properties.

In this work, the incorporation of polymer-grafted nanoparticles into self-healing photocurable elastomers at low loadings has been demonstrated as a viable strategy to subvert tradeoffs between stiffness and self-healing capacity. The mechanical reinforcement of PGNPs was shown to arise from the multivalent non-covalent interactions (hydrogen bonding and polymer entanglement) along polymer brush chains, which do not interfere with long-range polymer mobility. By tuning

PGNP structure and composition, the mechanical properties of nanocomposite materials could be tuned without compromising self-healing capacity. While functional limits still exist regarding critical filler loadings and brush density/size, judicious design of PGNP structural and compositional parameters should provide compatibility with a broad array of self-healing resins. Further, the straightforward integration of PGNP resins into a commercial DLP-based 3D printing process enables this strategy to be readily adapted to the fabrication of functional devices. Future studies exploring materials with stronger dynamic interactions are anticipated to enable even broader tunability in mechanical performance by adapting the method to different polymer and PGNP compositions. Additional work will also explore the healing of complex fracture geometries, addressing the influence of local stress on polymer network deformation and self-healing capacity.

Experimental Section

Materials

Unless otherwise noted, all reagents were used as received. Triethoxysilane (96%), tetraethoxysilane (99.9%), 1,6-hexanediol diacrylate (99%), and tin(ii) 2-ethylhexanoate (95%) were purchased from Alfa Aesar. Karstedt's catalyst (0.1 M in PDMS), 1,8-octanedithiol (97%), phenylbis(2,4,6-trimethylbenzoyl) phosphineoxide (BAPO) (99%), 2-Hydroxyethyl acrylate (2-HEA) (96%), and n-Butyl acrylate (nBA) (98%) were purchased from Sigma-Aldrich. Prior to their use in PGNP SI-ATRP reactions, the monomers were passed through a column of basic alumina to remove inhibitor. Bipyridine was purchased from Beantown Chemical. Anhydrous copper (ii) chloride (99+%) was purchased from Acros and stored as a stock solution in dimethylformamide (DMF) (20 mg/mL). 2-Bromoisobutyryl bromide (>98%) was purchased from

TCI America. Ammonium hydroxide (aqueous, 28-30 wt%), triethylamine (99%), and trifluoroacetic acid (TFA) (>97%) were purchased from Thermo Fisher Scientific. All solvents were of analytical grade and were used as received.

Synthesis of Self-healing Crosslinker TMSDA

The self-healing crosslinker ((Sulfonylbis(ethane-2,1-diyl)bis(sulfanediyl)bis(ethane-2,1-diyl)) diacrylate (TMSDA) was synthesized according to previous studies.⁴¹ A full synthetic procedure is available in the supporting information.

Synthesis of Surface-Tetherable ATRP Initiator

The synthesis of (2-bromo-2-methyl)propionyloxyhexyltriethoxysilane (BHE) was carried out in two separate steps according to previous studies.^{33–36} In brief, 2-bromoisobutyryl bromide and 5-hexen-1-ol were combined via esterification to form the intermediate 1-(2-bromo-2-methyl)propionyloxy-5-hexene (BPH), which was subsequently reacted with triethoxysilane via hydrosilylation to yield BHE. The initiator was stored in a dark cabinet until active use. See the supporting information for full synthetic details.

Synthesis of SiO₂ Nanoparticles with Surface-Tethered ATRP Initiator

Monodisperse SiO_2 nanoparticles were obtained via the Stöber process.^{42–44} Immediately following particle preparation, BHE was incrementally added in excess over a 24 h period to yield surface functionalized particles with diameters of ~ 50 and ~ 160 nm. See the supporting information for full synthetic details.

Synthesis and Characterization of Polymer-Grafted Nanoparticles

The PGNP brushes used in this study were grown directly from the BHE-functionalized nanoparitcle surfaces via surface-initiated atom transfer radical polymerization (SI-ATRP).^{35,45} A complete synthetic protocol is detailed in the supporting information as depicted in Scheme S1.

Preparation of mold-cured tensile testing samples

For typical control elastomer dog bones, 2-HEA and nBA were combined in a 4:1 wt:wt ratio in a 20 mL scintillation vial along with 1 phr TMSDA and 1 phr 1,8-octanedithiol. 0.5 phr BAPO was then added, and the vials were vigorously mixed to ensure dissolution. Aluminum foil was wrapped around the vials in order to protect the resins within from premature initiation via ambient light. The solutions were pipetted into 2 mm deep silicone dog bone molds and photopolymerized under high-intensity 365 nm UV light for 2 min. Samples were left to rest under ambient conditions for 3 days. Self-healing samples were then bisected with a razor blade and rejoined. Both cut and uncut samples were then placed in a convection oven at 90 °C for 24 h. After heat treating, specimens were removed from the oven and allowed to rest again under ambient conditions for 24 hours prior to mechanical characterization. Samples with multiple cut/heal cycles were cut again in the same spot after resting and the heat treatment was repeated.

Mechanical Characterization

Dog bone specimens were prepared in compliance with ASTM D 638 V. Tensile testing was performed on a Zwick-Roell BTC-EXMACRO equipped with a 10 N load cell and custom self-tightening specimen grips. Stress was calculated as force divided by initial cross-sectional area. Samples were strained at a rate of 50 mm/min until failure. Each resin composition was tested with a minimum of 3 specimens and all measurements were performed at 22 °C.

3D Printing

3D printing was performed with a custom-built DLP printer using a 405nm LED as the light source. The light intensity at the build surface is 6.7 mW/cm², as measured with a Thorlabs PM100USB detector. The layer height was set to 50 microns for all prints, and a layer exposure time of 4.2 seconds was used for each layer. The resin was lightly agitated (mild shaking by hand for a few seconds) before each print to ensure a homogeneous suspension of PGNPs. After printing parts were rinsed with IPA for 30 seconds, post-cured for 2-5 minutes in a 405 nm cure box, then transferred to a separate surface coated with silicone mold release spray to prevent adhesion.

Supporting Information

Full synthetic details, additional control experiments, and complete tensile measurement sets are available in the supporting information document.

Author Information

Corresponding Authors

Robert J. Macfarlane - Department of Materials Science and Engineering, Massachusetts
Institute of Technology, 77 Massachusetts Avenue, Cambridge, Massachusetts 02139, United
States

Carl J. Thrasher - Department of Materials Science and Engineering, Massachusetts Institute of Technology, 77 Massachusetts Avenue, Cambridge, Massachusetts 02139, United States

Authors

Griffen J. Desroches - Department of Chemistry, Massachusetts Institute of Technology, 77
Massachusetts Avenue, Cambridge, Massachusetts 02139, United States

Nicholas S. Diaco - Department of Mechanical Engineering, Massachusetts Institute of Technology, 77 Massachusetts Avenue, Cambridge, Massachusetts 02139, United States

Ibrahim O. Raji - Department of Chemistry and Biochemistry, Miami University, 651 E. High St., Oxford, OH 45056, United States

A. John Hart - Department of Mechanical Engineering, Massachusetts Institute of Technology, 77 Massachusetts Avenue, Cambridge, Massachusetts 02139, United States

Dominik Konkolewicz - Department of Chemistry and Biochemistry, Miami University, 651 E. High St., Oxford, OH 45056, United States

Author Contributions

The manuscript was written through contributions of all authors. All authors have given approval to the final version of the manuscript.

Notes

The authors declare no competing financial interest.

Acknowledgement

PGNP synthesis and characterization was funded by Tesa GMBH. Dynamic bonding chemistry development and synthesis was supported by NSF Award No. DMR- 1749730 to DK. This work was also supported by Department of Defense MURI Award N00014-23-1-2499 to AH and RM,

Shared Experimental Facilities at MIT, supported by NSF Award No. DMR 14-19807.

References:

- (1) Roppolo, I.; Caprioli, M.; Pirri, C. F.; Magdassi, S. 3D Printing of Self-Healing Materials. *Adv. Mater.* **2024**, *36* (9), 2305537. https://doi.org/10.1002/adma.202305537.
- (2) Zhu, G.; Houck, H. A.; Spiegel, C. A.; Selhuber-Unkel, C.; Hou, Y.; Blasco, E. Introducing Dynamic Bonds in Light-Based 3D Printing. *Adv. Funct. Mater.* **2024**, *34* (20), 2300456. https://doi.org/10.1002/adfm.202300456.
- (3) Terryn, S.; Brancart, J.; Lefeber, D.; Assche, G. V.; Vanderborght, B. Self-Healing Soft Pneumatic Robots. *Sci. Robot.* **2017**, *2* (9). https://doi.org/10.1126/scirobotics.aan4268.
- (4) Fang, Z.; Song, H.; Zhang, Y.; Jin, B.; Wu, J.; Zhao, Q.; Xie, T. Modular 4D Printing via Interfacial Welding of Digital Light-Controllable Dynamic Covalent Polymer Networks. *Matter* **2020**, *2* (5), 1187–1197. https://doi.org/10.1016/j.matt.2020.01.014.
- (5) J. Wallin, T.; H. Pikul, J.; Bodkhe, S.; N. Peele, B.; Murray, B. C. M.; Therriault, D.; W. McEnerney, B.; P. Dillon, R.; P. Giannelis, E.; F. Shepherd, R. Click Chemistry Stereolithography for Soft Robots That Self-Heal. *J. Mater. Chem. B* **2017**, *5* (31), 6249–6255. https://doi.org/10.1039/C7TB01605K.
- (6) Yu, K.; Xin, A.; Du, H.; Li, Y.; Wang, Q. Additive Manufacturing of Self-Healing Elastomers. *NPG Asia Mater.* **2019**, *11* (1), 1–11. https://doi.org/10.1038/s41427-019-0109-y.
- (7) Wang, W.; Liu, S.; Liu, L.; Alfarhan, S.; Jin, K.; Chen, X. High-Speed and High-Resolution 3D Printing of Self-Healing and Ion-Conductive Hydrogels via μCLIP. ACS Mater. Lett. 2023, 5 (6), 1727–1737. https://doi.org/10.1021/acsmaterialslett.3c00439.
- (8) Caprioli, M.; Roppolo, I.; Chiappone, A.; Larush, L.; Pirri, C. F.; Magdassi, S. 3D-Printed Self-Healing Hydrogels via Digital Light Processing. *Nat. Commun.* **2021**, *12* (1), 2462. https://doi.org/10.1038/s41467-021-22802-z.
- (9) Robinson, L. L.; Self, J. L.; Fusi, A. D.; Bates, M. W.; Read de Alaniz, J.; Hawker, C. J.; Bates, C. M.; Sample, C. S. Chemical and Mechanical Tunability of 3D-Printed Dynamic Covalent Networks Based on Boronate Esters. *ACS Macro Lett.* **2021**, *10* (7), 857–863. https://doi.org/10.1021/acsmacrolett.1c00257.
- (10) Sordo, F.; Mougnier, S.-J.; Loureiro, N.; Tournilhac, F.; Michaud, V. Design of Self-Healing Supramolecular Rubbers with a Tunable Number of Chemical Cross-Links. *Macromolecules* **2015**, *48* (13), 4394–4402. https://doi.org/10.1021/acs.macromol.5b00747.
- (11) Durand-Silva, A.; Cortés-Guzmán, K. P.; Johnson, R. M.; Perera, S. D.; Diwakara, S. D.; Smaldone, R. A. Balancing Self-Healing and Shape Stability in Dynamic Covalent Photoresins for Stereolithography 3D Printing. *ACS Macro Lett.* **2021**, *10* (4), 486–491. https://doi.org/10.1021/acsmacrolett.1c00121.
- (12) Zhang, B.; Digby, Z. A.; Flum, J. A.; Chakma, P.; Saul, J. M.; Sparks, J. L.; Konkolewicz, D. Dynamic Thiol–Michael Chemistry for Thermoresponsive Rehealable and Malleable Networks. *Macromolecules* **2016**, *49* (18), 6871–6878. https://doi.org/10.1021/acs.macromol.6b01061.

- (13) Wang, Z.; Cui, H.; Liu, M.; Grage, S. L.; Hoffmann, M.; Sedghamiz, E.; Wenzel, W.; Levkin, P. A. Tough, Transparent, 3D-Printable, and Self-Healing Poly(Ethylene Glycol)-Gel (PEGgel). *Adv. Mater.* **2022**, *34* (11), 2107791. https://doi.org/10.1002/adma.202107791.
- (14) Zhu, G.; Hou, Y.; Xiang, J.; Xu, J.; Zhao, N. Digital Light Processing 3D Printing of Healable and Recyclable Polymers with Tailorable Mechanical Properties. *ACS Appl. Mater. Interfaces* **2021**, *13* (29), 34954–34961. https://doi.org/10.1021/acsami.1c08872.
- (15) Wanasinghe, S. V.; Johnson, B.; Revadelo, R.; Eifert, G.; Cox, A.; Beckett, J.; Osborn, T.; Thrasher, C.; Lowe, R.; Konkolewicz, D. 3D Printable Adhesive Elastomers with Dynamic Covalent Bond Rearrangement. *Soft Matter* **2023**, *19* (26), 4964–4971. https://doi.org/10.1039/D3SM00394A.
- (16) Nevejans, S.; Ballard, N.; Fernández, M.; Reck, B.; García, S. J.; Asua, J. M. The Challenges of Obtaining Mechanical Strength in Self-Healing Polymers Containing Dynamic Covalent Bonds. *Polymer* **2019**, *179*, 121670. https://doi.org/10.1016/j.polymer.2019.121670.
- (17) Mei, V.; Schimmelpfennig, K.; Caravaca, E.; Colvin, S.; Lewis, C. L. Investigating the Structure–Property–Processing Relationship of Polycaprolactone-Based 3D Printed Self-Healing Polymer Blends. *ACS Appl. Polym. Mater.* **2024**, *6* (4), 2177–2187. https://doi.org/10.1021/acsapm.3c02628.
- (18) Appuhamillage, G. A.; Chartrain, N.; Meenakshisundaram, V.; Feller, K. D.; Williams, C. B.; Long, T. E. 110th Anniversary: Vat Photopolymerization-Based Additive Manufacturing: Current Trends and Future Directions in Materials Design. *Ind. Eng. Chem. Res.* 2019. https://doi.org/10.1021/acs.iecr.9b02679.
- (19) Thrasher, C. J.; Schwartz, J. J.; Boydston, A. J. Modular Elastomer Photoresins for Digital Light Processing Additive Manufacturing. *ACS Appl. Mater. Interfaces* **2017**, *9* (45), 39708–39716. https://doi.org/10.1021/acsami.7b13909.
- (20) Bagheri, A.; Bainbridge, C. W. A.; Engel, K. E.; Qiao, G. G.; Xu, J.; Boyer, C.; Jin, J. Oxygen Tolerant PET-RAFT Facilitated 3D Printing of Polymeric Materials under Visible LEDs. *ACS Appl. Polym. Mater.* **2020**. https://doi.org/10.1021/acsapm.9b01076.
- (21) Gauci, S. C.; Vranic, A.; Blasco, E.; Bräse, S.; Wegener, M.; Barner-Kowollik, C. Photochemically Activated 3D Printing Inks: Current Status, Challenges, and Opportunities. *Adv. Mater. n/a* (n/a), 2306468. https://doi.org/10.1002/adma.202306468.
- (22) Zhang, B.; De Alwis Watuthanthrige, N.; Wanasinghe, S. V.; Averick, S.; Konkolewicz, D. Complementary Dynamic Chemistries for Multifunctional Polymeric Materials. *Adv. Funct. Mater.* **2022**, *32* (8), 2108431. https://doi.org/10.1002/adfm.202108431.
- (23) Li, X.; Yu, R.; He, Y.; Zhang, Y.; Yang, X.; Zhao, X.; Huang, W. Self-Healing Polyurethane Elastomers Based on a Disulfide Bond by Digital Light Processing 3D Printing. *ACS Macro Lett.* **2019**, 1511–1516. https://doi.org/10.1021/acsmacrolett.9b00766.
- (24) Yu, K.; Du, H.; Xin, A.; Lee, K. H.; Feng, Z.; Masri, S. F.; Chen, Y.; Huang, G.; Wang, Q. Healable, Memorizable, and Transformable Lattice Structures Made of Stiff Polymers. *NPG Asia Mater.* **2020**, *12* (1), 1–16. https://doi.org/10.1038/s41427-020-0208-9.
- (25) Gomez, E. F.; Wanasinghe, S. V.; Flynn, A. E.; Dodo, O. J.; Sparks, J. L.; Baldwin, L. A.; Tabor, C. E.; Durstock, M. F.; Konkolewicz, D.; Thrasher, C. J. 3D-Printed Self-Healing Elastomers for Modular Soft Robotics. *ACS Appl. Mater. Interfaces* **2021**. https://doi.org/10.1021/acsami.1c06419.

- (26) J. Dodo, O.; O. Raji, I.; J. Arny, I.; P. Myers, C.; Petit, L.; Walpita, K.; Dunn, D.; J. Thrasher, C.; Konkolewicz, D. Dynamic Polymer Nanocomposites towards Strain Sensors and Customizable Resistors. *RSC Appl. Polym.* **2023**, *1* (1), 30–45. https://doi.org/10.1039/D3LP00012E.
- (27) Wu, Y.; Zeng, Y.; Chen, Y.; Li, C.; Qiu, R.; Liu, W. Photocurable 3D Printing of High Toughness and Self-Healing Hydrogels for Customized Wearable Flexible Sensors. *Adv. Funct. Mater.* **2021**, *31* (52), 2107202. https://doi.org/10.1002/adfm.202107202.
- (28) Guo, B.; Ji, X.; Chen, X.; Li, G.; Lu, Y.; Bai, J. A Highly Stretchable and Intrinsically Self-Healing Strain Sensor Produced by 3D Printing. *Virtual Phys. Prototyp.* **2020**, *15* (sup1), 520–531. https://doi.org/10.1080/17452759.2020.1823570.
- (29) Street, D. P.; Mah, A. H.; Ledford, W. K.; Patterson, S.; Bergman, J. A.; Lokitz, B. S.; Pickel, D. L.; Messman, J. M.; Stein, G. E.; Kilbey, S. M. I. Tailoring Interfacial Interactions via Polymer-Grafted Nanoparticles Improves Performance of Parts Created by 3D Printing. *ACS Appl. Polym. Mater.* **2020**, *2* (3), 1312–1324. https://doi.org/10.1021/acsapm.9b01195.
- (30) Liang, J.; Francoeur, M.; Williams, C. B.; Raeymaekers, B. Curing Characteristics of a Photopolymer Resin with Dispersed Glass Microspheres in Vat Polymerization 3D Printing. *ACS Appl. Polym. Mater.* **2023**, *5* (11), 9017–9026. https://doi.org/10.1021/acsapm.3c01479.
- (31) Rossegger, E.; Höller, R.; Hrbinič, K.; Sangermano, M.; Griesser, T.; Schlögl, S. 3D Printing of Soft Magnetoactive Devices with Thiol-Click Photopolymer Composites. *Adv. Eng. Mater.* **2023**, *25* (7), 2200749. https://doi.org/10.1002/adem.202200749.
- (32) Shah, M.; Ullah, A.; Azher, K.; Ur Rehman, A.; Juan, W.; Aktürk, N.; Sami Tüfekci, C.; U. Salamci, M. Vat Photopolymerization-Based 3D Printing of Polymer Nanocomposites: Current Trends and Applications. *RSC Adv.* **2023**, *13* (2), 1456–1496. https://doi.org/10.1039/D2RA06522C.
- (33) Desroches, G.; Wang, Y.; Kubiak, J.; Macfarlane, R. Crosslinking of Pressure-Sensitive Adhesives with Polymer-Grafted Nanoparticles. *ACS Appl. Mater. Interfaces* **2022**, *14* (7), 9579–9586. https://doi.org/10.1021/acsami.1c22997.
- (34) Kubiak, J. M.; Macfarlane, R. J. Forming Covalent Crosslinks between Polymer-Grafted Nanoparticles as a Route to Highly Filled and Mechanically Robust Nanocomposites. *Adv. Funct. Mater.* **2019**, *29* (44), 1905168. https://doi.org/10.1002/adfm.201905168.
- (35) Ohno, K.; Morinaga, T.; Koh, K.; Tsujii, Y.; Fukuda, T. Synthesis of Monodisperse Silica Particles Coated with Well-Defined, High-Density Polymer Brushes by Surface-Initiated Atom Transfer Radical Polymerization. *Macromolecules* **2005**, *38* (6), 2137–2142. https://doi.org/10.1021/ma048011q.
- (36) Yan, J.; Pan, X.; Schmitt, M.; Wang, Z.; Bockstaller, M. R.; Matyjaszewski, K. Enhancing Initiation Efficiency in Metal-Free Surface-Initiated Atom Transfer Radical Polymerization (SI-ATRP). *ACS Macro Lett.* **2016**, *5* (6), 661–665. https://doi.org/10.1021/acsmacrolett.6b00295.
- (37) Kubiak, J. M.; Macfarlane, R. J. Polymer-Grafted Nanoparticles as Single-Component, High Filler Content Composites via Simple Transformative Aging. *Adv Funct Mater* **2022**, 32 (6), 2107139.
- (38) Desroches, G. J.; Gatenil, P. P.; Nagao, K.; Macfarlane, R. J. Mechanical Reinforcement of Waterborne Latex Pressure-Sensitive Adhesives with Polymer-Grafted Nanoparticles. *J. Polym. Sci.* **2024**, *62* (4), 743–752. https://doi.org/10.1002/pol.20230355.

- (39) Wisse, E.; Govaert, L. E.; Meijer, H. E. H.; Meijer, E. W. Unusual Tuning of Mechanical Properties of Thermoplastic Elastomers Using Supramolecular Fillers. *Macromolecules* **2006**, *39* (21), 7425–7432. https://doi.org/10.1021/ma060986i.
- (40) #3DBenchy. #3DBenchy. https://www.3dbenchy.com/ (accessed 2024-05-27).
- (41) Chakma, P.; Wanasinghe, S. V.; Morley, C. N.; Francesconi, S. C.; Saito, K.; Sparks, J. L.; Konkolewicz, D. Heat- and Light-Responsive Materials Through Pairing Dynamic Thiol—Michael and Coumarin Chemistry. *Macromol. Rapid Commun.* **2021**, *42* (18), 2100070. https://doi.org/10.1002/marc.202100070.
- (42) Stöber, W.; Fink, A.; Bohn, E. Controlled Growth of Monodisperse Silica Spheres in the Micron Size Range. *J. Colloid Interface Sci.* **1968**, *26* (1), 62–69. https://doi.org/10.1016/0021-9797(68)90272-5.
- (43) Lei, X.; Yu, B.; Cong, H.-L.; Tian, C.; Wang, Y.-Z.; Wang, Q.-B.; Liu, C.-K. Synthesis of Monodisperse Silica Microspheres by a Modified Stöber Method. *Integr. Ferroelectr.* 2014, 154 (1), 142–146. https://doi.org/10.1080/10584587.2014.904651.
- (44) Huang, Y.; Pemberton, J. E. Synthesis of Uniform, Spherical Sub-100nm Silica Particles Using a Conceptual Modification of the Classic LaMer Model. *Colloids Surf. Physicochem. Eng. Asp.* **2010**, *360* (1), 175–183. https://doi.org/10.1016/j.colsurfa.2010.02.031.
- (45) Dong, H.; Zhu, M.; Yoon, J. A.; Gao, H.; Jin, R.; Matyjaszewski, K. One-Pot Synthesis of Robust Core/Shell Gold Nanoparticles. *J. Am. Chem. Soc.* **2008**, *130* (39), 12852–12853. https://doi.org/10.1021/ja8038097.